

Total inelastic-scattering cross sections by optical-potential methods

Philip W. Coulter

Department of Physics and Astronomy, The University of Alabama, University, Alabama 35486

W. R. Garrett

Chemical Physics Section, Health and Safety Research Division, Oak Ridge National Laboratory, Oak Ridge, Tennessee 37830

(Received 6 October 1980)

Total excitation cross sections for electrons scattering from atomic hydrogen are calculated by using a complex optical potential. Distorted-wave propagators as well as free-particle propagators are used in computing the optical potential. It is found that using an attractive potential to generate the propagator results in poorer agreement with experiment than using a free-particle propagator. The effect of neglecting coupling between excited target states in computing the optical potential is also studied. It is concluded that it necessary to include coupling between excited target states if the calculation is to be reliable.

I. INTRODUCTION

In a recent paper¹ we used the complex optical-potential method of Feshbach² to study electron scattering by atomic hydrogen in the energy region below which the Born approximation provides an adequate description of scattering phenomena. Differential cross sections below the first excitation threshold were computed and found to be in reasonable agreement with experimental data. Total excitation and ionization cross sections were calculated for electrons with energies up to 5 Ry (68 eV). Our calculated ionization cross sections were not in good agreement with experiment,^{3,4} but they compared favorably with ionization cross sections obtained by Geltman, Rudge, and Seaton⁵ using the Born, Born-Oppenheimer, and Born-exchange approximations. Only the Born-exchange results were in better agreement with experiment than our results. More recently, McCarthy and McDowell⁶ obtained a good fit to the experimental ionization cross sections by using an optical model with an adjustable parameter. There was no adjustable parameter in the calculations of Ref. 1.

Electron impact excitation of ground-state hydrogen atoms to the 2s and 2p states is of fundamental interest. There have been many attempts to obtain these excitation cross sections theoretically.⁷⁻¹⁰ These results have been reviewed by Moiseiwitsch and Smith¹¹ and Williams and Willis.¹² Kingston, Fon, and Burke¹³ used a 1s-2s-2p close-coupling approximation for low partial waves and a unitarized Born approximation for higher partial waves to calculate 1s → 2s and 1s → 2p excitation cross sections. They believe their results to be accurate above 100 eV; however, their calculated excitation cross sections do not agree well with experiment below 54.4 eV.

In this paper we have extended our previous

calculations to include 1s → 2s and 1s → 2p excitation cross sections. We made three approximations in computing the optical-model potential. The distorted-wave (diagonal) approximation, in which direct couplings between excited states are neglected, was used. Exchange effects in excited states were neglected, and a free-particle propagator was used for electrons interacting with excited target states. In the present study we have computed the excitation cross sections using these same approximations. We have also investigated the effects of using distorted-wave propagators and including interchannel coupling in a phenomenological manner.

Using the approximations in Ref. 1 we found that the 1s → 2s excitation cross sections were too large for incident electron energies from 2 Ry up to 5 Ry. Our 1s → 2p excitation cross sections are too large below about 4 Ry and smaller than the experimental data above 4 Ry. In order to test the sensitivity of these results to the form of the propagator, we repeated the calculations using a Coulomb propagator for the excited states. In this case the electron is propagated in the field of the nucleus. The true description of the multi-channel scattering should lie somewhere between these two extremes. This modification increased the disagreement with experimental data. The 1s → 2s excitation cross section got larger at all energies while the 1s → 2p excitation cross section got larger at low energies and smaller at high energies. Other more realistic interactions (non-Coulomb) were also used with similar results. Thus it seems unlikely that the accuracy of the calculation can be significantly improved by simply introducing a distorted-wave propagator generated by an attractive potential.

Interchannel coupling can be accounted for phenomenologically by using a complex potential to describe the propagation of an electron inter-

acting with an excited target state.¹⁴ The theory for this method is worked out in detail in two appendices. We were able to obtain significant improvement in the calculated cross sections by using this approach to include interchannel coupling, but more work needs to be done before this technique can be used with any confidence. These calculations indicate that neglecting interchannel coupling in computing the optical potential is not a good approximation.

We have not made any attempt to examine the effect of neglecting antisymmetrization in excited states. McCarthy and McDowell⁶ suggest that an accurate optical potential must include second-order exchange contributions at least at energies below 50 eV. In a practical calculation of the type undertaken here it is almost impossible to include second-order exchange effects without using a local approximation for the exchange interaction. Exchange effects could then be included by using a suitably modified effective interaction for electrons interacting with excited target states.

The formalism will be presented in the next section. The results of the calculations will be presented in Sec. III and compared with other theoretical calculations and experimental data where possible. Our conclusions are discussed in Sec. IV.

II. FORMALISM

Since we neglect exchange effects except in the elastic channel we will ignore exchange in presenting the formalism and introduce the direct-channel exchange contribution at the end. Then we have

$$H(\vec{r}_1, \vec{r}_2)\Psi(\vec{r}_1, \vec{r}_2) = E\Psi(\vec{r}_1, \vec{r}_2), \quad (1)$$

where

$$H(\vec{r}_1, \vec{r}_2) = H_1(\vec{r}_1) + H_2(\vec{r}_2) + V(\vec{r}_1, \vec{r}_2). \quad (2)$$

H_1 and H_2 describe the target and projectile, respectively, and V describes the target-projectile interaction. For electron-hydrogen scattering with a fixed nucleus

$$\begin{aligned} H_1(\vec{r}_1) &= -\nabla_1^2 - \frac{2}{r_1}, \\ H_2(\vec{r}_2) &= -\nabla_2^2, \\ V(\vec{r}_1, \vec{r}_2) &= -\frac{2}{r_2} + \frac{2}{|\vec{r}_1 - \vec{r}_2|}. \end{aligned} \quad (3)$$

We use units where \hbar and a_0 (the Bohr radius) are 1 and the unit of energy is the rydberg.

We expand the total wave function in terms of target eigenstates as

$$\Psi(\vec{r}_1, \vec{r}_2) = \sum_n \phi_n(\vec{r}_1)\chi_n(\vec{r}_2),$$

where

$$H_1(\vec{r}_1)\phi_n(\vec{r}_1) = \epsilon_n\phi_n(\vec{r}_1). \quad (4)$$

\sum indicates a sum over the discrete target eigenstates plus a sum over the continuum target eigenstates. By taking the integral

$$\int d^3r_1 \phi_k^*(\vec{r}_1)H(\vec{r}_1, \vec{r}_2)\Psi(\vec{r}_1, \vec{r}_2),$$

we obtain a set of coupled equations:

$$\sum_n [E_k \delta_{kn} - H_{kn}(\vec{r}_2)]\chi_n(\vec{r}_2) = 0, \quad (5)$$

$$H_{kn}(\vec{r}_2) = H_2(\vec{r}_2)\delta_{kn} + V_{kn}(\vec{r}_2), \quad (6)$$

$$V_{kn}(\vec{r}_2) = \int \phi_k(\vec{r}_1)V(\vec{r}_1, \vec{r}_2)\phi_n(\vec{r}_1)d^3r_1, \quad (7)$$

$$E_k = E - \epsilon_k. \quad (8)$$

Since H_2 is the kinetic-energy operator we can also write H_{kn} as

$$H_{kn}(\vec{r}_2) = T(\vec{r}_2)\delta_{kn} + V_{kn}(\vec{r}_2).$$

We define the free-particle Green's function or propagator by

$$[E_k - T(\vec{r})]G_{kn}^{(0)}(\vec{r}, \vec{r}') = \delta_{kn}\delta(\vec{r} - \vec{r}'). \quad (9)$$

We will denote the ground-state target eigenstate by ϕ_0 so that

$$[E_0 - H_{00}(\vec{r}_2)]\chi_0(\vec{r}_2) = \sum_k' H_{0k}(\vec{r}_2)\chi_k(\vec{r}_2) \quad (10)$$

where $\sum_k' = \sum_{k \neq 0}$. The excited-state wave function can be found from ($k \neq 0$)

$$\sum_n' [E_k \delta_{kn} - H_{kn}(\vec{r}_2)]\chi_n(\vec{r}_2) = H_{k0}(\vec{r}_2)\chi_0(\vec{r}_2). \quad (11)$$

We now define an exact Green's function for the system with the elastic channel omitted ($k, m, n \neq 0$):

$$\sum_n' [E_k \delta_{kn} - H_{kn}(\vec{r}_2)]G_{nm}(\vec{r}_2, \vec{r}_2') = \delta_{km}\delta(\vec{r}_2 - \vec{r}_2'). \quad (12)$$

G_{nm} can be found from

$$\begin{aligned} G_{nm}(\vec{r}_2, \vec{r}_2') &= G_{nm}^{(0)}(\vec{r}_2, \vec{r}_2') \\ &+ \sum_{k,l}' \int d^3r_1 G_{nk}^{(0)}(\vec{r}_2, \vec{r}_1)V_{kl}(\vec{r}_1)G_{lm}(\vec{r}_1, \vec{r}_2'). \end{aligned} \quad (13)$$

Thus for $k \neq 0$,

$$\chi_k(\vec{r}_2) = \sum_n' \int d^3r_2' G_{kn}(\vec{r}_2, \vec{r}_2')H_{n0}(\vec{r}_2')\chi_0(\vec{r}_2') \quad (14)$$

and the elastic channel wave function satisfies the nonlocal equation

$$[E_0 - H_{00}(\vec{r}_2)]\chi_0(\vec{r}_2) = \int d^3r'_2 V_0(\vec{r}_2, \vec{r}'_2)\chi_0(\vec{r}'_2), \quad (15)$$

where

$$V_0(\vec{r}_2, \vec{r}'_2) = \sum_{k,l} H_{0k}(\vec{r}_2) G_{kl}(\vec{r}_2, \vec{r}'_2) H_{l0}(\vec{r}'_2). \quad (16)$$

Here V_0 is the exact optical potential for this unsymmetrized system. In the diagonal approximation we set $G_{kl} = 0$ if $k \neq l$ so that

$$V_0(\vec{r}_2, \vec{r}'_2) = \sum_k H_{0k}(\vec{r}_2) G_{kk}(\vec{r}_2, \vec{r}'_2) H_{k0}(\vec{r}'_2). \quad (17)$$

In Ref. 1 we also replaced G_{kk} by the free-particle propagator $G_{kk}^{(0)}$ in evaluating V_0 .

We must still make a partial wave expansion of χ_0 . The details of this are presented by Alton *et al.*¹⁵ and the modification needed to include exchange effects in the direct channel is given in Ref. 1. Also, we describe in the following section (and in Appendix A) a method of estimating the effect of including nondiagonal terms in the above formalism.

III. RESULTS AND DISCUSSION

The excitation cross section to any particular excited state can be calculated (in the diagonal approximation) from¹⁶

$$\sigma_{0 \rightarrow k} = -\frac{2m}{\hbar^2 k} \int d^3r d^3r' \chi_0(\vec{r}) V_k^{(A)}(\vec{r}, \vec{r}') \chi_0(\vec{r}'), \quad (18)$$

where $V_k^{(A)}(r, r')$ is the absorptive (imaginary) part of the optical potential which results from the excited-state k alone

$$V_k^{(A)} = \text{Abs}[H_{0k}(\vec{r}) G_{kk}(r, r') H_{k0}(\vec{r}')]. \quad (19)$$

We first computed the $1s \rightarrow 2s$ and $1s \rightarrow 2p$ excitation cross sections using the same approximations as in Ref. 1. The results of this calculation are shown in Figs. 1 and 2.

In Fig. 1 we plot the $1s \rightarrow 2s$ excitation cross section as a function of incident electron energy from threshold up to 5 Ry. For comparison we also plot the excitation cross section found from the $1s \rightarrow 2s \rightarrow 2p$ close-coupling approximation.¹³ The experimental data,¹⁷ uncorrected for cascade effects, are also shown. Since the data are uncorrected for cascade effects, the true $1s \rightarrow 2s$ excitation cross section will be less than the data. The experimental cross section can be approximated by $\sigma(1s \rightarrow 2s) + 0.23\sigma(1s \rightarrow 3p)$.¹⁸ The $1s \rightarrow 3p$ excitation cross section has been calculated by Syms *et al.*¹⁹ If their results are used, the experimental data of Kauppila, Ott, and Fite¹⁷

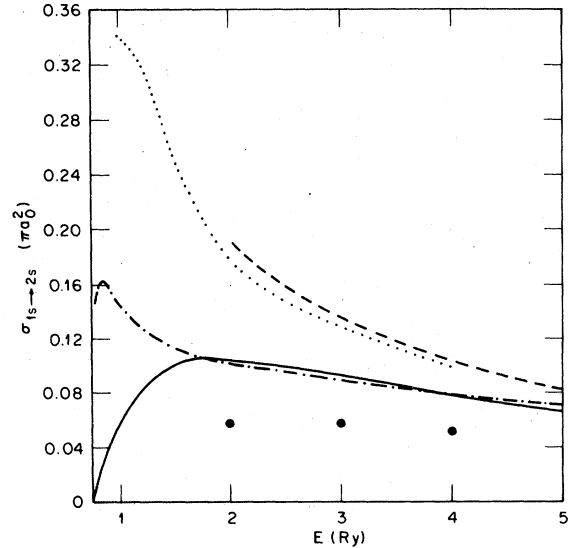


FIG. 1. $1s \rightarrow 2s$ excitation cross section as a function of incident electron energy. The solid line describes the cross section obtained by using a free-particle propagator to compute the optical potential. The dashed curve is found by using the $1s \rightarrow 2s \rightarrow 2p$ close-coupling method (Ref. 13). The dash-dot curve shows the experimental results (Ref. 17), which are uncorrected for cascading into the $2s$ level (see text). The \bullet indicates the cross sections found by using an imaginary potential to generate the propagator (see text).

should be reduced by approximately $0.3\pi a^2$ in the energy range from 2 to 5 Ry in order to obtain the $1s \rightarrow 2s$ excitation cross section. We also show the $1s \rightarrow 2s$ excitation cross section which is found

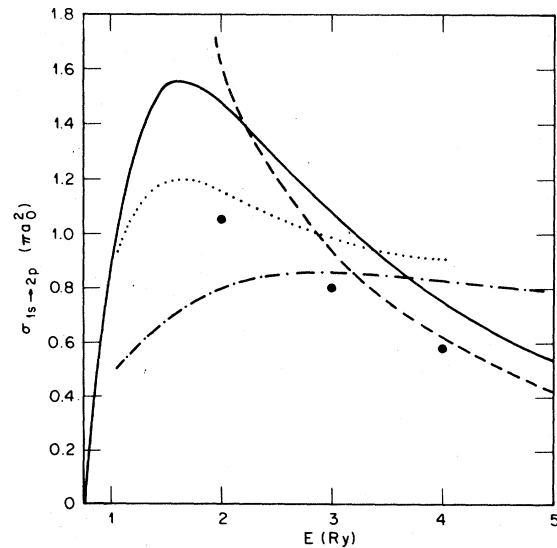


FIG. 2. $1s \rightarrow 2p$ excitation cross section as a function of incident electron energy. The notation is the same as in Fig. 1. The experimental curve is from Refs. 20 and 21.

by using a Coulomb propagator instead of a free-particle propagator. The agreement with experiment is much worse for this case.

In Fig. 2 we plot the $1s-2p$ excitation cross section as a function of incident electron energy. Again we show the results of the $1s-2s-2p$ close-coupling calculation¹³ as well as the experimental data.^{20,21} In our calculation we include only 12 partial waves. With reference to the calculation of Burke, Schey, and Smith²² we estimate that about $0.1\pi a_0^2$ should be added to our result at 4 Ry. This correction for neglecting higher partial waves would improve the agreement of our calculation with experiment at energies above 4 Ry. The correction for higher partial waves is more important for the $1s-2p$ excitation cross section than for the $1s-2s$ excitation cross section since the $1s, 2p$ coupling is relatively long range. We also show the $1s-2p$ excitation cross section which is obtained by using a Coulomb propagator. Again we see that the use of a Coulomb propagator rather than a free-particle propagator does not improve the agreement with experimental data.

In Fig. 3 we plot the ionization cross section as a function of incident electron energy. The experimental curve which is shown is the average experimental result.^{3,4} Again we see that using a Coulomb propagator leads to poorer agreement with experiment. We also used propagators generated by shielded Coulomb potentials and we tried varying the effective charge in the interaction. None of these attempts led to better fits than those found by using a free-particle propagator.

Contrary to our expectations we found that the use of a distorted-wave propagator to compute the optical potential does not lead to better agreement with experiment. We conclude that it is unlikely

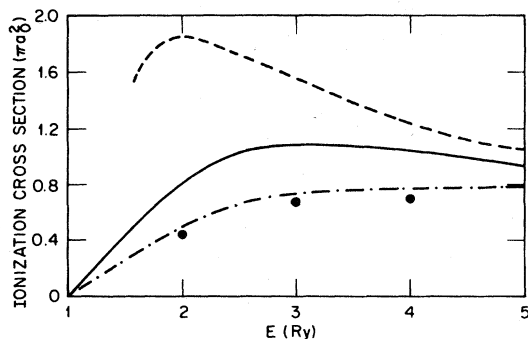


FIG. 3. Ionization cross section as a function of incident electron energy. The notation is the same as in Fig. 1. The experimental curve is the average of the results of Refs. 3 and 4.

that one can introduce a simple, real distorting potential for excited states and hope to improve the calculation significantly. A possible reason for this is that the neglected interchannel coupling between excited states of the system is not at all negligible in the total scattering interaction. We have tried to gain additional insight into the importance of interchannel coupling through an approximate treatment of these effects. We show in Appendix A how one may include this interchannel coupling in a phenomenological way by using a complex distorting potential in determining the propagator. Equations (18) and (19) can be used only if the distorting potential is real. The modification which must be made for a complex distorting potential is discussed in Appendix B. We found that making the distorting potential complex can lead to significant improvements in the calculations.

In order to assess the efficacy of a complex distorting potential in representing interchannel coupling, we chose a simple parametrized function, purely imaginary, in the form

$$u(\vec{r}) = -2i\alpha \frac{e^{-r/r_0}}{r}. \quad (20)$$

This form for $u(r)$ was chosen simply for convenience, since our aim was not to try to reproduce any realistic potentials. This function has readily interpretable range and strength parameters. For $\alpha=1$, the magnitude of $u(r)$ near $r=0$ is the same as the Coulomb potential between the electron and the nucleus. Thus, it is easy to compare the strength of the assumed potential with other interaction terms. The results of a limited number of calculations utilizing the form (2) are shown as the solid circles in Figs. 1-3. The results shown in the figures were obtained with $r_0=5a_0$ and $\alpha=0.2$. We used the same $u(r)$ for each excited target state. In a more elaborate calculation different distorting potentials could be used in different channels. We did not attempt an extensive parameter search to obtain the best fit to the cross-section data. The results shown here represent the best of several choices of α in the range 0.1-0.5. We also examined a complex distorting potential with an attractive real part. With this form for $u(r)$ the size of the imaginary part had to be increased in order to obtain the reasonable agreement with the data. Even for strongly attractive potentials, comparable to the electron-nucleus interaction, the required values of α did not exceed 0.4. On the basis of this limited study it is apparent that interchannel coupling plays a non-negligible role in determining low-energy inelastic-scattering cross sections, and that these effects can be represented

reasonably well through use of a fairly weak complex distortion potential in the propagator. We made no attempt to vary α or r_0 with energy to obtain a good fit to the data over the entire energy range, though such a study would give some insight into the energy dependence of the role of interchannel coupling near thresholds for inelastic collisions.

IV. SUMMARY AND CONCLUSIONS

We have extended the investigation in Ref. 1 of the optical-potential method for atomic excitation and ionization. We have calculated $1s \rightarrow 2s$ and $1s \rightarrow 2p$ excitation cross sections and investigated the effect of two of the approximations made in Ref. 1 on the calculations. We find that using non-plane-wave propagators to compute the optical potential seems to lead to poorer agreement between the calculations and experiment. This is true as long as the potential generating the propagator is attractive. It was noted coincidentally that in the present context a repulsive potential can lead to enhanced agreement with experiment, but we know of no justification for the use of such a representation in the present problem. More work needs to be done in this area.

We also investigated the effect of making the diagonal approximation in computing the optical potential. Interchannel coupling can be accounted for by using a complex potential to generate the

propagator. This technique led to generally improved agreement with experiment. This result at least indicates that a reliable microscopic calculation of the optical potential must include direct coupling between excited target states in some fashion.

We have not attempted to include exchange effects in excited states in these calculations or to study the effect of their omission in the formalism. Exchange effects will clearly play an important role in determining the effective potential to be used in generating the propagators. Before this type of calculation of the optical potential can be expected to be reliable and practical, we must have a method for generating a reasonable complex potential to describe the propagation of electrons interacting with excited target states.

ACKNOWLEDGMENTS

One of us (P.W.C.) was supported in part by a consultantship with the Chemical Physics Section of the Health and Safety Research Division of Oak Ridge National Laboratory and by a grant from The University of Alabama Research Grants Committee. Research at Oak Ridge is funded by the Department of Energy under Contract No. W-7405-Eng-26 with Union Carbide Corporation. The computations were done at the Charles Seebek Computer Center at The University of Alabama.

APPENDIX A

Using a complex potential for electrons propagating in the field of an excited target state can be justified by following a procedure similar to that used in Sec. II. Suppose we want to find a particular wave function $\chi_m(r)$ ($m \neq 0$). Then

$$[E_m - H_{mm}(\vec{r}_2)]\chi_m(\vec{r}_2) = H_{m0}(\vec{r}_2)\chi_0(\vec{r}_2) + \sum_k'' H_{mk}(\vec{r}_2)\chi_k(\vec{r}_2), \quad (A1)$$

where $\sum_n'' \equiv \sum_{n \neq 0, m}$. For $p \neq m, 0$ we have

$$\sum_p'' [\delta_{kp}E_k - H_{kp}(\vec{r}_2)]\chi_p(\vec{r}_2) = H_{k0}(\vec{r}_2)\chi_0(\vec{r}_2) + H_{km}(\vec{r}_2)\chi_m(\vec{r}_2). \quad (A2)$$

Now we find a Green's function for the reduced system in which both 0 and m are omitted:

$$G'_{pq}(\vec{r}_2, \vec{r}_2') = G_{pq}^{(0)}(\vec{r}_2, \vec{r}_2') + \sum_{k, n}'' d^3 r_1 G_{pk}^{(0)}(\vec{r}_2, \vec{r}_1) V_{kn}(\vec{r}_1) G'_{nq}(\vec{r}_1, \vec{r}_2'). \quad (A3)$$

Then

$$\chi_k(\vec{r}_2) = \sum_n'' \int d^3 r_2' G'_{kn}(\vec{r}_2, \vec{r}_2') [H_{n0}(\vec{r}_2')\chi_0(\vec{r}_2') + H_{nm}(\vec{r}_2')\chi_m(\vec{r}_2')]. \quad (A4)$$

If we use Eq. (A4) in Eq. (A1) we obtain

$$\begin{aligned} [E_m - H_{mm}(\vec{r}_2)]\chi_m(\vec{r}_2) - \sum_{k, n}'' \int d^3 r_2' H_{mk}(\vec{r}_2) G'_{kn}(\vec{r}_2, \vec{r}_2') H_{nm}(\vec{r}_2') \chi_m(\vec{r}_2') \\ = H_{m0}(\vec{r}_2)\chi_0(\vec{r}_2) + \sum_{k, n}'' \int d^3 r_2' H_{mk}(\vec{r}_2) G'_{kn}(\vec{r}_2, \vec{r}_2') H_{n0}(\vec{r}_2') \chi_0(\vec{r}_2'). \end{aligned} \quad (A5)$$

If we define

$$V_m(\vec{r}_2, \vec{r}'_2) = \sum_{k,n}'' H_{mk}(\vec{r}_2) G'_{kn}(\vec{r}_2, \vec{r}'_2) H_{nm}(\vec{r}'_2) \quad (\text{A6})$$

and neglect the last term on the right in Eq. (A5) we get, in this approximation,

$$\begin{aligned} [E_m - H_{mm}(\vec{r}_2)] \chi_m(\vec{r}_2) - \int d^3r'_2 V_m(\vec{r}_2, \vec{r}'_2) \chi_m(\vec{r}'_2) \\ = H_{m0}(\vec{r}_2) \chi_0(\vec{r}_2). \end{aligned} \quad (\text{A7})$$

In the present study we further assume that V_m can be replaced by a local equivalent potential so that

$$[E_m - H_{mm}(\vec{r}_2) - V_{Lm}(\vec{r}_2)] \chi_m(\vec{r}_2) = H_{m0}(\vec{r}_2) \chi_0(\vec{r}_2). \quad (\text{A8})$$

V_{Lm} will have an imaginary part whenever G_{kn} has an imaginary part. Thus V_{Lm} will be complex whenever any excited state other than 0 or m is energetically accessible.

APPENDIX B

We establish a generalization to Eq. (18) and illustrate the added labor involved in the use of the "distorted" propagator in the calculation of inelastic cross sections. In order to calculate the total excitation cross section from channel 0 to channel m we will use Eq. (A8) to solve for χ_m :

$$\chi_m(\vec{r}_2) = \int d^3r'_2 G_m(\vec{r}_2, \vec{r}'_2) H_{m0}(\vec{r}'_2) \chi_0(\vec{r}'_2), \quad (\text{B1})$$

$$[E_m - H_{mm}(\vec{r}_2) - V_{Lm}(\vec{r}_2)] G_m(\vec{r}_2, \vec{r}'_2) = \delta(\vec{r}_2 - \vec{r}'_2). \quad (\text{B2})$$

The propagator can be written as

$$G_m(\vec{r}_2, \vec{r}'_2) = \frac{1}{r_2 r'_2} \sum_{\lambda\mu} g_\lambda(k_m, r_2, r'_2) Y_{\lambda\mu}(\hat{r}_2) Y_{\lambda\mu}^*(\hat{r}'_2), \quad (\text{B3})$$

where $k_m^2 = E_m$ in our units. Assuming for simplicity that the total potential in channel m is a com-

$$G_m(\vec{r}_2, \vec{r}'_2) \xrightarrow{r_2 \rightarrow \infty} -\frac{e^{ik_m r_2}}{r_2} \frac{1}{\sqrt{k_m r'_2}} \sum_{\lambda\mu} e^{-i\lambda\pi/2} F_\lambda(k_m, r'_2) Y_{\lambda\mu}^*(\hat{r}'_2) Y_{\lambda\mu}(\hat{r}_2). \quad (\text{B10})$$

Also

$$\chi_m(\vec{r}_2) \xrightarrow{r_2 \rightarrow \infty} \frac{e^{ik_m r_2}}{r_2} F_m(\hat{r}_2),$$

where

$$F_m(\hat{r}_2) = -\frac{1}{\sqrt{k_m}} \sum_{\lambda\mu} \int d^3r'_2 e^{i\lambda\pi/2} \frac{F_\lambda(k_m, r'_2)}{r'_2} H_{m0}(\vec{r}'_2) Y_{\lambda\mu}(\hat{r}_2) Y_{\lambda\mu}^*(\hat{r}'_2) \chi_0(\vec{r}'_2). \quad (\text{B11})$$

The excitation cross section is given by

$$\sigma_{0 \rightarrow m} = \frac{k_m}{k_0} \int |F_m(\hat{r}_2)|^2 d\Omega_2. \quad (\text{B12})$$

plex central potential, the g_λ satisfy the equations

$$\left(\frac{d^2}{dr^2} + k^2 - \frac{\lambda(\lambda+1)}{r^2} - u(r) \right) g_\lambda(k, r, r') = \delta(r - r'). \quad (\text{B4})$$

Here $u(r)$ is obtained by combining V_{Lm} and the potential in H_{mm} . g_λ can be computed from

$$\begin{aligned} g_\lambda(k, r, r') = g_\lambda^{(0)}(k, r, r') \\ + \int_0^\infty g_\lambda^{(0)}(k, r, r'') u(r'') g_\lambda(k, r'', r') dr''. \end{aligned} \quad (\text{B5})$$

$g_\lambda^{(0)}$ is the free-particle propagator and we have assumed that the potential has a finite range. $g_\lambda^{(0)}$ can be computed in the usual manner:

$$g_\lambda^{(0)}(k, r, r') = -f_\lambda(k, r_\zeta) h_\lambda(k, r_\zeta). \quad (\text{B6})$$

r_ζ (r_ζ) is the larger (smaller) of r, r' . Also $f_\lambda(k, r) = \sqrt{k} r j_\lambda(kr)$ and $h_\lambda(k, r) = \sqrt{k} r [-n_\lambda(kr) + i j_\lambda(kr)]$, where j_λ and n_λ are spherical Bessel functions of the first and second kind, respectively. We further note that asymptotically $f_\lambda(k, r) \sim (1/\sqrt{k}) \sin(kr - \lambda\pi/2)$, and $h_\lambda(k, r) \sim (1/\sqrt{k}) e^{i(kr - \lambda\pi/2)}$.

To obtain the total excitation cross section we must find the asymptotic form of χ_m . We note that asymptotically

$$g_\lambda(k, r, r') \xrightarrow{r \rightarrow \infty} -h_\lambda(k, r) F_\lambda(k, r'), \quad (\text{B7})$$

where

$$\begin{aligned} F_\lambda(k, r) = f_\lambda(k, r) \\ + \int_0^\infty f_\lambda(k, r') u(r') g_\lambda(k, r', r) dr', \end{aligned} \quad (\text{B8})$$

and F_λ satisfies the radial wave equation

$$\left(\frac{d^2}{dr^2} + k^2 - \frac{\lambda(\lambda+1)}{r^2} - u(r) \right) F_\lambda(k, r) = 0. \quad (\text{B9})$$

Using Eqs. (B3), (B6), and the asymptotic forms of f and h , we see that

Thus

$$\sigma_{0 \rightarrow m} = -\frac{1}{k_0} \int d^3r_2 d^3r_2' \chi_0^*(\vec{r}_2) V_m^{(A)}(\vec{r}_2, \vec{r}_2') \chi_0(r_2'), \quad (\text{B13})$$

where $V_m^{(A)}$ is defined to be

$$V_m^{(A)}(\vec{r}_2, \vec{r}_2') = -H_{m0}(\vec{r}_2) \left(\sum_{\lambda\mu} \frac{F_\lambda^*(k_m, r_2) F_\lambda(k_m, r_2')}{r_2 r_2'} Y_{\lambda\mu}(\hat{r}_2) Y_{\lambda\mu}^*(\hat{r}_2') \right) H_{0m}(\vec{r}_2'). \quad (\text{B14})$$

If the potential u is real, Eq. (B14) and Eq. (19) are identical. When utilizing a distorting potential we note that numerical solutions are required not only for the scattered waves, but also for the complex radial components F_λ of the distorted propagator.

We have assumed that the potentials were local in this appendix. It is straightforward to generalize the present derivation to account for nonlocal potentials.

¹P. W. Coulter and W. R. Garrett, Phys. Rev. A 18, 1902 (1978).

²H. Feshbach, Ann. Phys. (N.Y.) 5, 357 (1958).

³W. L. Fite and R. T. Brackman, Phys. Rev. 112, 1141 (1958).

⁴R. L. F. Boyd and A. Boksenberg, in *Proceedings of the Fourth International Conference on Ionization Phenomena in Gases, Uppsala, 1959*, edited by N. R. Nilsson (North-Holland, Amsterdam, 1960), Vol. I, p. 529.

⁵S. Geltman, M. R. H. Rudge, and M. J. Seaton, Proc. Phys. Soc. London 81, 375 (1963).

⁶I. E. McCarthy and M. R. C. McDowell, J. Phys. B 5, 3775 (1979).

⁷P. G. Burke, H. M. Schey, and K. Smith, Phys. Rev. 129, 1258 (1963).

⁸P. G. Burke and A. J. Taylor, Proc. Phys. Soc. London 88, 549 (1966).

⁹P. G. Burke, A. J. Taylor, and S. Omonde, Proc. Phys. Soc. London 92, 345 (1967); J. Phys. B 1, 325 (1968).

¹⁰P. G. Burke, S. Ormonde, and W. Whitaker, Proc. Phys. Soc. London 92, 319 (1967).

¹¹B. L. Moiseiwitsch and S. J. Smith, Rev. Mod. Phys. 40, 238 (1968).

¹²J. F. Williams and B. A. Willis, J. Phys. B 7, L61 (1974).

¹³A. E. Kingston, W. C. Fon, and P. G. Burke, J. Phys. B 9, 605 (1976).

¹⁴P. W. Coulter and G. R. Satchler, Nucl. Phys. A 293, 269 (1977).

¹⁵G. D. Alton, W. R. Garrett, M. Reeves, and J. E. Turner, Phys. Rev. A 6, 2138 (1972).

¹⁶P. W. Coulter, Phys. Rev. A 18, 1908 (1978).

¹⁷W. E. Kauppila, W. R. Ott, and W. R. Fite, Phys. Rev. A 1, 1099 (1970).

¹⁸D. G. Hummer and M. J. Seaton, Phys. Rev. Lett. 6, 471 (1961).

¹⁹R. F. Syms, M. R. C. McDowell, L. A. Morgan, and V. P. Myerscough, J. Phys. B 8, 2817 (1975).

²⁰J. W. McGowan, J. F. Williams, and E. K. Curley, Phys. Rev. 180, 132 (1969).

²¹R. L. Long, D. M. Cox, and S. J. Smith, J. Res. Natl. Bur. Stand. 72A, 521 (1968).

²²P. G. Burke, H. M. Schey, and K. Smith, Phys. Rev. 129, 1258 (1963).